JOURNAL OF MATERIALS SCIENCE 7 (1972) 895–908

Crystallization of lithium magnesium zinc silicates

Part 2 *Phase equilibria and the crystallization of glasses in the system Li_4SiO_4-Mg_2SiO_4-Zn_2SiO_4-SiO_2*

A. R. WEST, F. P. GLASSER
Department of Chemistry, University of Aberdeen, Meston Walk, Old Aberdeen, Aberdeen, Scotland

Subsolidus phase equilibria in the system Li_4SiO_4-Zn_2SiO_4-Mg_2SiO_4-SiO_2 have been studied and seventeen quaternary subsolidus phase volumes identified. The crystalline orthosilicate phases are solid solutions, and their compositions or ranges of composition in the various quaternary volumes have been determined. Perspective drawings are used to show the relationship between quaternary subsolidus phase volumes at about 850° C. An unusual feature of the phase distribution is that all quaternary compositions, even those highest in silica content, will yield a ternary γ-type orthosilicate phase at equilibrium. This phase is structurally related to Li_3PO_4. Examples are given of the calculation of the phase composition at equilibrium for various quaternary volumes.

The crystallization of quaternary glasses is compared with the equilibrium phase diagram. At crystallization temperatures approaching the solidus, the equilibrium phases are readily obtained. At lower temperatures, about 500 to 600° C, metastable phases are formed. These include lithium disilicate having a variable Li : Si ratio, the Proto-β phase which has a wurtzite-like structure and metastable orthosilicates. These phases persist indefinitely at lower temperatures, but readily convert to the equilibrium phases on reheating to higher temperatures.

1. Introduction

Many of the crystalline phases which occur in this system have compositions which are essentially fixed, and their properties are comparatively well known: Li_2SiO_3 and $MgSiO_3$ are examples. The crystal chemistry of several of the orthosilicates and the phase equilibria in the system Li_4SiO_4-Zn_2SiO_4-Mg_2SiO_4 have only recently been described [1-3]. Complexities arise due to polymorphism and wide ranges of solid solution formation amongst the orthosilicates. The orthosilicates are important crystallization products of glass-ceramics whose compositions lie in the Li_2O-MgO-ZnO-SiO_2 system, even though most liquids which readily form glasses will have silica contents which are substantially greater than 50 mol % SiO_2.* The properties of the orthosilicate phases are very sensitive to the phase composition, and their occurrence in quaternary compositions can, therefore, only be predicted if the equilibria and important non-equilibria in the quaternary system are known. One purpose of the present study has been to determine these fundamental data. Usually, the study of a four-component oxide system is a formidable task, but in the present study, the volume of experimental work necessary was reduced by taking full advantage of the existing data on the limiting ternary systems; these data were used to predict certain features of the subsolidus phase relations. While these predictions must always be subject to actual experimental verification, this procedure enables a reduction in the necessary experimental work, thus permitting such systems to be explored quickly, yet accurately.

*All percentages in this paper are given in mol %.

2. Experimental

Compositions within the quaternary system were prepared using two sets of starting material. In one series, sintered compositions on the join Li_2ZnSiO_4-Li_2MgSiO_4 were mixed with silica in a 1:1 molar ratio. The mixtures were sintered at about 870°C for several days; approximately half (1 to 2 g) of each batch was then melted at 1200 to 1300°C for 10 to 12 h and quenched to form a glass. A second series of mixtures of bulk composition (35 mol % Li_2O, 25% (Zn + Mg)O, 40% SiO_2) was prepared using Li_4SiO_4, $Li_2(Zn, Mg)SiO_4$ and SiO_2 as starting materials; each mixture was reacted at about 870°C. The initial sinterings and the preparation of glasses were all carried out in platinum crucibles using electrically-heated muffle furnaces. Small lumps of glass wrapped in gold foil were crystallized in muffle furnaces: temperatures shown in the Tables are accurate to ± 25°C.

Samples were examined optically using a petrographic microscope. Powder X-ray patterns were recorded with either a Guinier-de-Wolff focusing camera or a Philips PW 1051 diffractometer.

3. Results and Discussion

3.1. The ternary systems Li_4SiO_4-Zn_2SiO_4-SiO_2 and Li_4SiO_4-Mg_2SiO_4-SiO_2

With a knowledge of phase relations on the orthosilicate joins, more accurate ternary phase diagrams can be constructed. Both these systems have been studied previously [4-6], but need correction or additions. Figs. 1 and 2 show the 850°C isothermal sections through both systems, as determined in the present study. In the absence of any new ternary phases, the general shape of these diagrams could be predicted from data given in the literature together with corrections introduced from the previous studies of the orthosilicate joins [1, 3], but sufficient ternary compositions were prepared to confirm that the phase relations shown in Figs. 1 and 2 were, in fact, experimentally observed; the results are included in Table I.

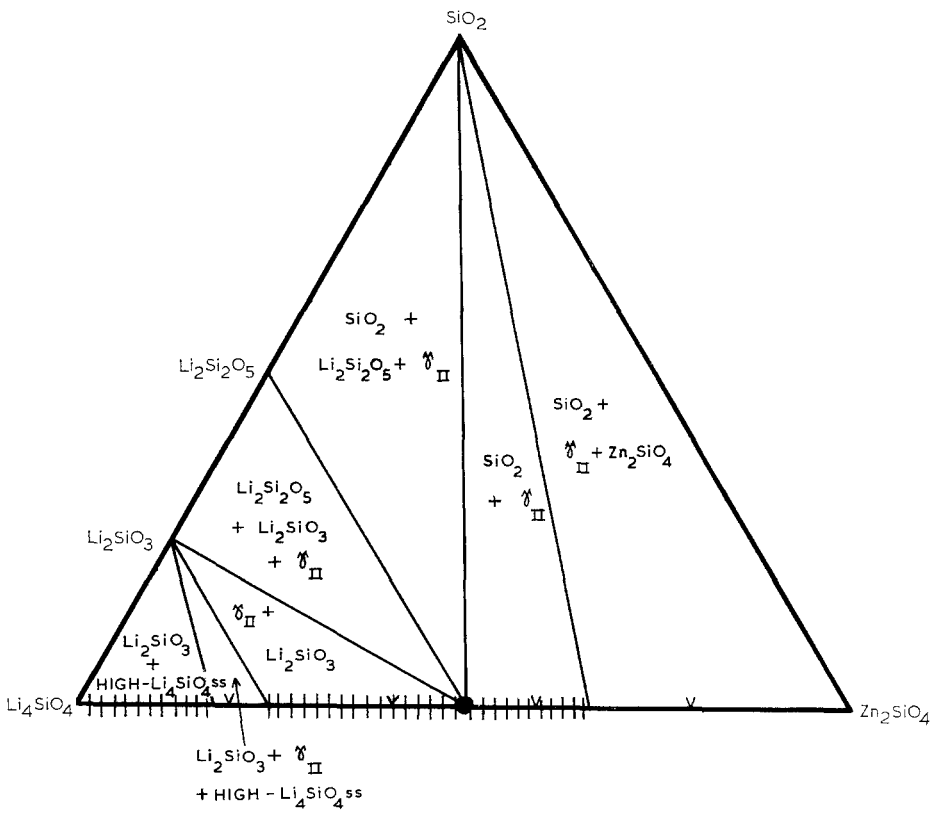

Figure 1 Subsolidus equilibria in the system Li_4SiO_4-Zn_2SiO_4-SiO_2 at about 850°C. Compositions on the orthosilicate join are in mol %. γ_{II} is the high-temperature form of solid solutions based on Li_2ZnSiO_4.

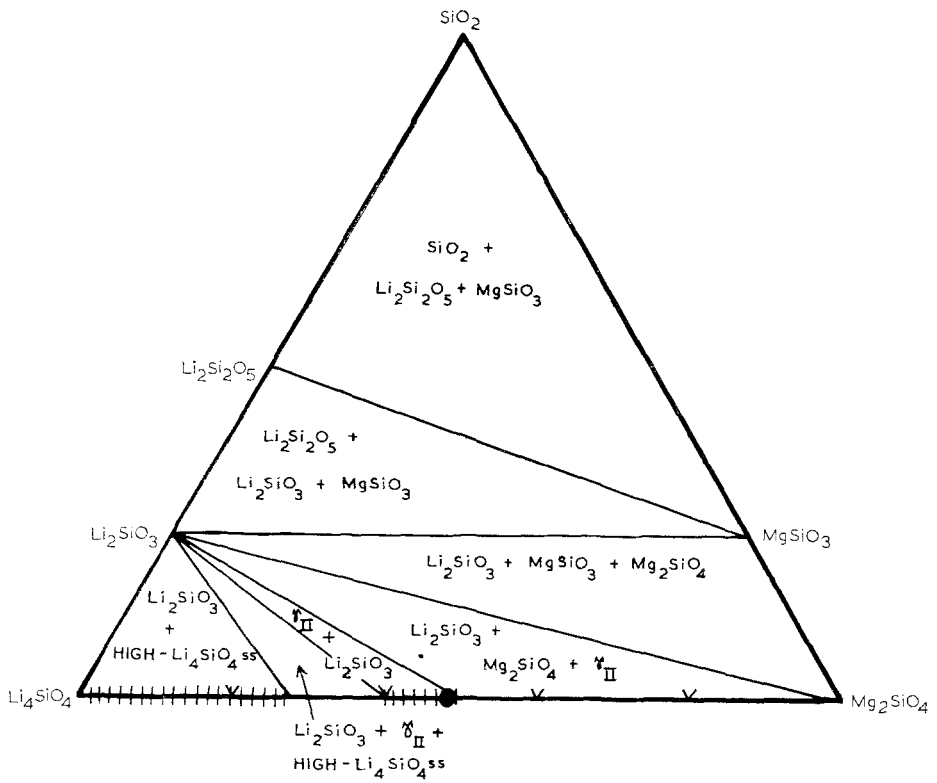

Figure 2 Subsolidus equilibria in the system Li_4SiO_4-Mg_2SiO_4-SiO_2 at about 850°C. Compositions on the orthosilicate join are in mol %. γ_{II} is the high-temperature form of solid solutions based on Li_2MgSiO_4.

Differences between the crystal chemistry of zinc and magnesium can readily be seen by comparing the two isothermal sections. Although the orthosilicates Li_2ZnSiO_4 and Li_2MgSiO_4 are very similar in their crystal chemistry (indeed they are completely miscible at higher temperatures) Zn_2SiO_4 and Mg_2SiO_4 are not isostructural and show only limited mutual solubility; moreover, no zinc counterpart of $MgSiO_3$ occurs. Further differences arise because, in the magnesium system, the join Mg_2SiO_4-Li_2SiO_3 is a stable entity, whereas in the zinc-containing system, Zn_2SiO_4 and Li_2SiO_3 are not compatible. This hypothetical join is, instead, crossed by other stable joins: that between Li_2ZnSiO_4 and SiO_2 is especially important in controlling the phase distribution in the zinc-containing system.

A further isothermal section at 650°C, Fig. 3, was studied to show how, in the zinc-containing system, SiO_2 can coexist with either β- or γ- or mixtures of β- and γ-orthosilicate phases. The equilibria on other isothermal sections are readily predicted with the aid of these data. Moreover, the sequences of metastable phase changes known to occur in the orthosilicates [2, 3] are not generally influenced by the presence of other phases, so that the sequences of metastable orthosilicate phase changes could also be incorporated into a series of metastable ternary isothermal sections. These would be based on the general features of the stable phase diagram, but modified as necessary by the principal metastable equilibria known to occur in the orthosilicate phases.

3.2. The ternary system Zn_2SiO_4-Mg_2SiO_4-SiO_2

Segnit and Holland [7] studied the phase equilibria in the system MgO-ZnO-SiO_2. The Zn_2SiO_4, Mg_2SiO_4 and $MgSiO_3$ compositions each give rise to a series of solid solutions. At subsolidus temperatures, willemite and its magnesium-containing solid solutions were found to coexist with $MgSiO_3$ and a small range of (Mg, Zn)SiO_3 solid solutions. Consequently, most glass-forming compositions fell within the

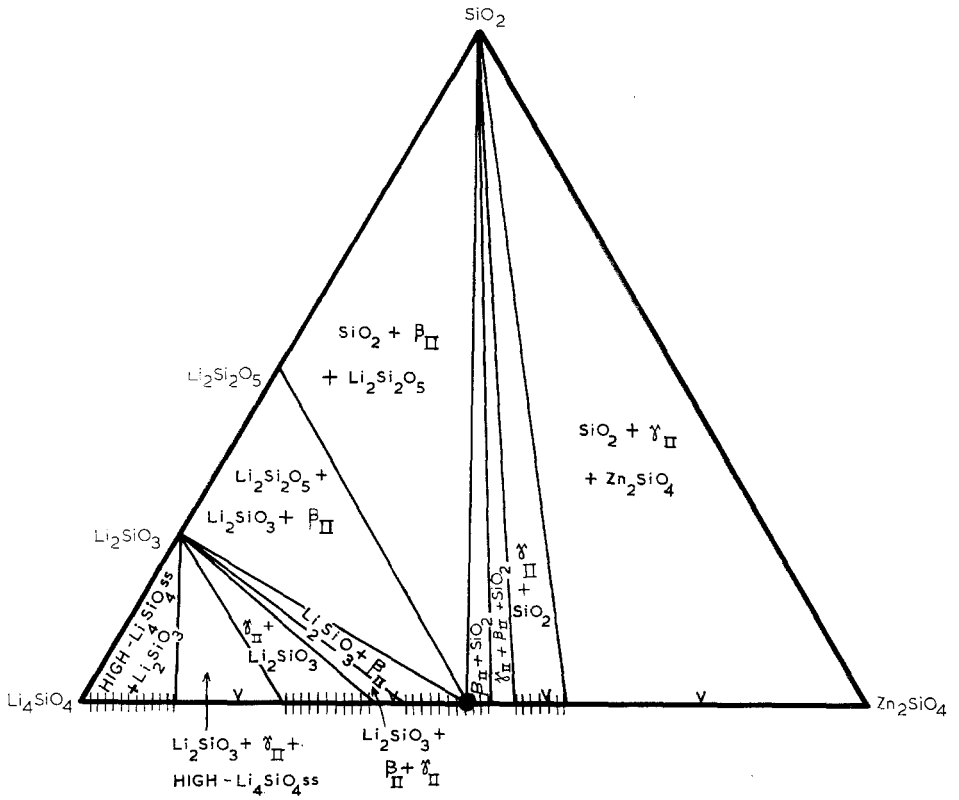

Figure 3 Subsolidus equilibria in the system Li_4SiO_4-Zn_2SiO_4-SiO_2 at about 650° C. Orthosilicate compositions are in mol %. β_{II} and γ_{II} are solid solution polymorphs based on Li_2ZnSiO_4.

three-phase triangle (SiO_2 + $MgSiO_3$ solid solution + magnesium-free Zn_2SiO_4). The refractive indices of the willemite solid solutions crystallized on the join willemite-forsterite were found to range from $\epsilon = 1.71_5$, $\omega = 1.68_5$ at at Zn_2SiO_4, to $\epsilon = 1.67_5$, $\omega = 1.65$ at the magnesium-rich limits of solid solution.

In the present study, a few experiments have been carried out to check these compatibility relations, especially amongst those compositions containing SiO_2 as one of the phases. These new data have necessitated some important revisions to Segnit and Holland's phase diagram.

In one experiment, a mixture whose composition lay within the triangle (Mg_2SiO_4 solid solution + Zn_2SiO_4 solid solution + $MgSiO_3$ solid solution) was prepared, using Mg_2SiO_4, Zn_2SiO_4 and SiO_2 as starting materials. After reacting at about 1400° C for six days, the mixture contained large quantities of magnesium meta- and orthosilicates and zinc orthosilicate: the magnesium/zinc ratios of these phases were not determined. Only trace amounts of silica remained and no glass was observed microscopically. This result confirms the finding [7] that no forsterite composition within this system may coexist with silica. However, a subsequent experiment showed that the range of willemite solid solutions coexists with silica and not, as was reported earlier, with $MgSiO_3$. In this experiment, a composition on the tie line (Zn_2SiO_4 solid solution-SiO_2), again prepared from Mg_2SiO_4, Zn_2SiO_4 and SiO_2, was reacted at 1400° C for six days. By X-ray analysis and optical microscopy, the products of reaction were willemite, cristobalite and glass. The refractive indices of the willemite crystals lay between $\epsilon = 1.68$, and $\omega = 1.66$, indicating their composition to be close to the magnesium-rich limits of solid solution. Although no direct subsolidus results for this composition were obtained—reaction was found to be extremely slow at about 1200° C—it is probable that, if magnesium-rich willemite solid solution and silica are compatible just above the solidus, they will also coexist below the solidus. It was not

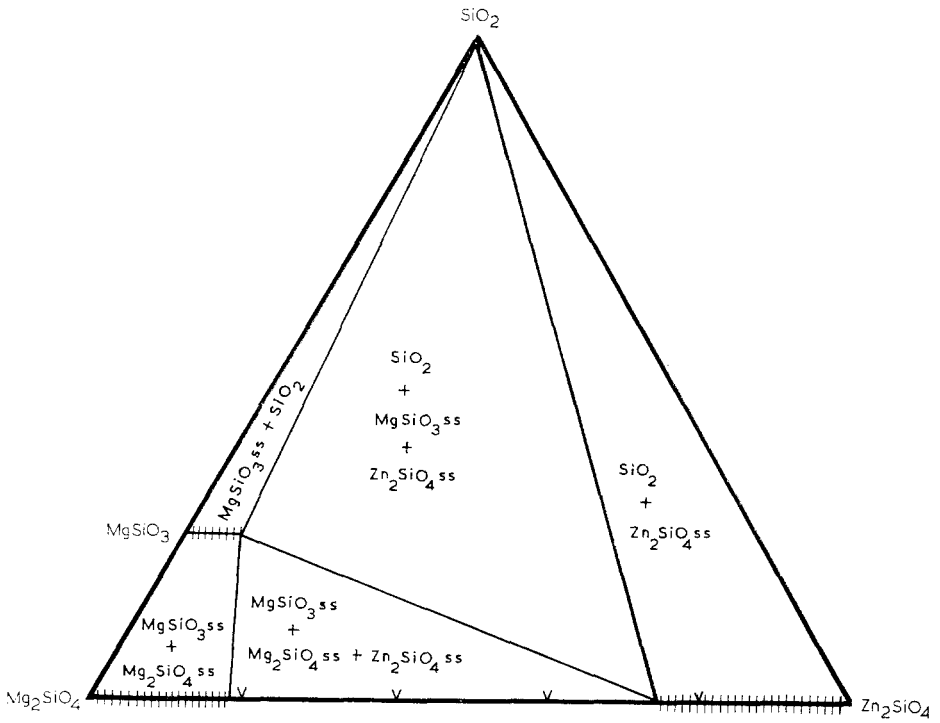

Figure 4 Subsolidus equilibria in the system Zn_2SiO_4-Mg_2SiO_4-SiO_2 at about 1200°C. Orthosilicate compositions are in mol %.

determined whether the magnesium metasilicate solid solutions coexist primarily with the willemite phase at its magnesium-rich limit of solid solution, or with the range of forsterite solid solutions. The latter alternative seems more likely. Fig. 4 thus includes a number of important corrections to the phase diagram shown by Segnit and Holland.

3.3. The ternary system Li_4SiO_4-Zn_2SiO_4-Mg_2SiO_4

The subsolidus equilibria taken from [3] are shown in Fig. 5, which depicts the isothermal section at 850 to 900°C.

3.4. The quaternary system Li_4SiO_4-Zn_2SiO_4-Mg_2SiO_4-SiO_2

The subsolidus equilibria in the bounding ternary faces of this system are shown in Figs. 1 to 5. In the absence of any quaternary phases or solid solutions, it is possible to make several deductions as to which phases will be compatible in the quaternary system. However, because of the dissimilarity between the ternary faces Li_4SiO_4-Zn_2SiO_4-SiO_2 and Li_4SiO_4-Mg_2SiO_4-SiO_2, and the complexity of the ternary orthosilicate system, a limited number of experiments are needed both to confirm these predictions and also to determine the solid solution compositions. The results of heat-treatment experiments involving both sintering and the crystallization of glass at subsolidus temperatures are given in Table I. From these data, the existence of most of the quaternary volumes could be either demonstrated or deduced. They are listed in Table II. Figs. 6 to 8 show in perspective the positions of these volumes at about 800 to 850°C, a temperature which is slightly below the minimum solidus temperature of 875 ± 25°C.

It is difficult to calculate the relationship between the bulk composition of a given mixture and the amounts of the various phases present, using these perspective drawings. Fig. 9 is constructed to facilitate this calculation for all compositions containing greater than 66.7% SiO_2 and also for some of the more basic

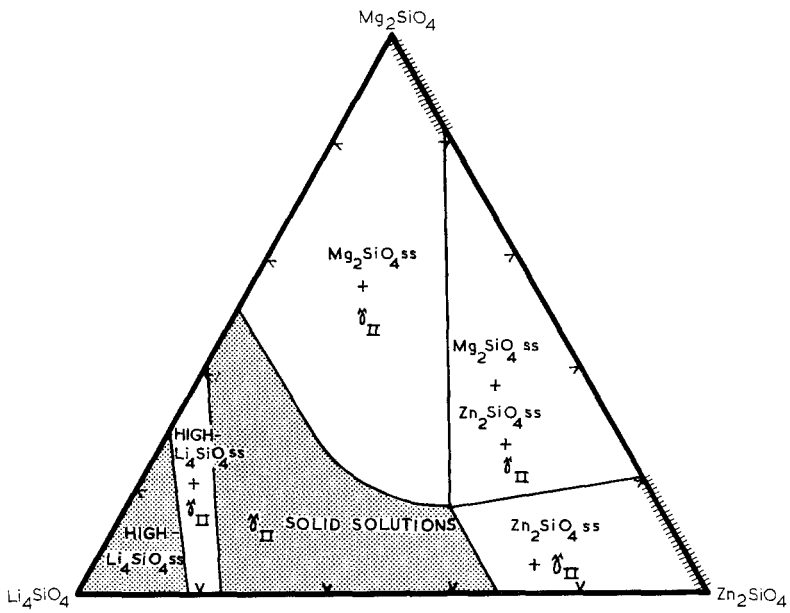

Figure 5 Subsolidus equilibria in the system Li_4SiO_4-Zn_2SiO_4-Mg_2SiO_4 at about 900°C. Compositions are in mol %.

TABLE I Results of heating experiments in the system Li_4SiO_4-Zn_2SiO_4-Mg_2SiO_4-SiO_2

Composition	Treatment	Phases present
10 Li_2O:9 ZnO:1 MgO:20 SiO_2 ..	900°, 1 day*	γ_0 + t − LS_2 + Cr + Q
	900°, 5 days*	,,
10 Li_2O:8ZnO:2 MgO:20 SiO_2 ..	900°, 1 day*	γ_0 + t − LS_2 + Cr + Q
	900°, 5 days*	,,
	540°, 16 days	Proto-β
	660°, 12h	,,
	790°, 12h	γ_0 + t − LS_2 + Q
	660°, 860°, 18h	,,
10 Li_2O:7 ZnO:3 MgO:20 SiO_2 ..	900°, 1 day*	γ_0 + t − LS_2 + T + Cr
	900°, 5 days*	γ_0 + t − LS_2 + Cr + Q
	870°, 5 days*	γ_0 + t − LS_2 + Q
	540°, 16 days	Proto-β
	620°, 4h	,,
	620, 660°, 4h	,,
	660°, 12h	γ_0 + Proto-β
	660°, 780°, 3h	γ_0 + t − LS_2 + Q
10 Li_2O:6 ZnO:4 MgO:20 SiO_2 ..	900°, 1 day*	γ_0 + T + Glass
	870°, 5 days*	γ_0 + Q + LS_2 + t − MS[a]
	540°, 16 days	Proto-β
	560°, 1 day	,,
	560°, 620°, 4h	,,
	560°, 620°, 660°, 3h	Proto-β + β_{II}
	660°, 12h	γ_0
	780°, 3h	γ_0 + Q + LS_2
	660°, 860°, 18h	γ_0 + Q + LS_2 + t − MS

TABLE I continued

10 Li_2O:5 ZnO:5 MgO:20 SiO_2 ..	870°, 5 days*	γ_0 + LS_2 + MS + Q
	540°, 16 days	Proto-β
	620°, 4h	,,
	620°, 660°, 3h	γ_0 + Proto-β
	660°, 12h	γ_0
	660°, 860°, 18h	γ_0 + LS_2 + MS + Q
	740°, 12h	,,
10 Li_2O:2 ZnO:8 MgO:20 SiO_2 ..	540°, 16 days	Proto-β + LS_2
	620°, 4h	,,
	620°, 660°, 3h	LS_2 + β_{II}
	660°, 12h	LS_2 + t − LS + γ_0 + MS
	780°, 12h	LS_2 + LS + γ_0 + MS
	660°, 860°, 18h	,,
10 Li_2O:10 MgO:20 SiO_2 ..	500°, 20h	Glass
	540°, 16 days	LS_2 + Proto-β
	620°, 4h	,,
	660°, 12h	LS + MS + t − LS_2
	660°, 860°, 18h	,,
14 Li_2O:6 ZnO:4MgO:16 SiO_2 ..	850, 4 days*	LS + LS_2 + γ_0
14 Li_2O:5 ZnO:5 MgO:16 SiO_2 ..	850°, 4 days*	LS + LS_2 + γ_0 + MS
14 Li_2O:3. 5 ZnO:6.5 MgO:16 SiO_2	850°, 1 day*	LS + LS_2 + γ_0 + MS
	850°, 2 days*	LS + LS_2 + γ_0 + MS + M_2S
	880°, 4 days*	LS + γ_0^d + MS + t − M_2S
14 Li_2O:2 ZnO:8 MgO:16 SiO_2 ..	850°, 4 days*	LS + γ_0^c + M_2S
6 Li_2O:1 ZnO:13 SiO_2	550°	LS_2
	550°, 640°	LS_2 + t − β − phase
	650°, 21 days	LS_2 + β_I + Q
6 Li_2O:2 ZnO:12 SiO_2 ..	550°	LS_2 + Proto-β
	550°, 640°	,,
	550°, 640°, 730°	LS_2 + β_I + Q
5 Li_2O:2 ZnO:13 SiO_2 ..	550°	LS_2^b + t − β − phase
	550°, 640°	,,
	550°, 640°, 730°	LS_2 + β_I + Q
4 Li_2O:4 ZnO:12 SiO_2 ..	540°, 16 days	Proto-β
	550°, 640°	β_{II}
	550°, 640°, 730°	β_I + Q + Cr
5 Li_2O:4 ZnO:11 SiO_2 ..	540°, 16 days	Proto-β
4 Li_2O:3 ZnO:13 SiO_2	540°, 16 days	LS_2^b + Proto-β
3 Li_2O:3 ZnO:14 SiO_2	540°, 16 days	Proto-β
4 Li_2O:5 ZnO:11 SiO_2	540°, 16 days	Proto-β + β_{II}
	600°, 700°	γ_0
3 Li_2O:4 ZnO:13 SiO_2 ..	540°, 16 days	β_{II}
	650°, 21 days	γ_0 + Cr + Q
3 Li_2O:5 ZnO:8 SiO_2 ..	540°, 16 days	β_{II}
	600°, 700°, 7 days	C- or C′-Li, Zn orthosilicate
3 Li_2O:6 ZnO:11 SiO_2 ..	540°, 16 days	t − β_{II}
2 Li_2O:7 ZnO:11 SiO_2 ..	550°, 640°	γ_{II} + t − Z_2S
	650°, 21 days	Z_2S + Cr + C′ − Li, Zn orthosilicate
2 Li_2O:1 ZnO:2 SiO_2 ..	900°, 28 days*	γ_0 + LS + t − LS_2
11 Li_2O:1 ZnO:8 SiO_2 ..	850°, 12h*	LS + L_2Sss + t − Q

Notes

*For these experiments, crystalline starting materials were used; for the remaining experiments, glass was the starting material.

[continued over

Notes on Table I continued
Cr – Cristobalite, Q – Quartz, T – Tridymite, t–; a trace of
LS_2 – $Li_2Si_2O_5$, LS – Li_2SiO_3, MS – $MgSiO_3$, M_2S – Mg_2SiO_4, Z_2S – Zn_2SiO_4, L_2Sss – Li_4SiO_4 solid solution.
[a] – The $MgSiO_3$ phase may contain a small amount of zinc in solid solution. It always crystallized as the rhombic enstatite modification.
[b] – From the appearance of the X-ray powder pattern, the disilicate phase appears to contain some excess SiO_2 in solid solution [8].
[c] – Estimated γ_0 composition (from $2\theta_{(0\,0\,2)}$)$Li_2Zn_{0.4}Mg_{0.6}SiO_4$.
[d] – Estimated γ_0 composition (from $2\theta_{(0\,0\,2)}$)$Li_2Zn_{0.45}Mg_{0.55}SiO_4$.
Although no ternary compositions within the system Li_4SiO_4-Mg_2SiO_4-SiO_2 were prepared, the appearance of Li_2SiO_3 in Li_4SiO_4 solid solution and γ-phase compositions heated at high temperatures, which had lost "Li_2O" by volatilization was considered sufficient to demonstrate the existence of two- and three-phase triangles containing Li_2SiO_3 and an orthosilicate(s).

TABLE II Subsolidus phase relations in the system Li_4SiO_4-Zn_2SiO_4-Mg_2SiO_4-SiO_2

Volumes of compatible phases (with compositions)	Shown in Fig.
*Li_4SiO_4 s.s. (Li_4SiO_4-a-b) + Li_2SiO_3	6
*Li_4SiO_4 s.s. (a-b) + Li_2SiO_3 + γ (c-d)	6
*Li_2SiO_3 + γ (c-d-h-g-f-e)	6, 8
*Li_2SiO_3 + $Li_2Si_2O_5$ + γ (e-f)	6
*$Li_2Si_2O_5$ + SiO_2 + γ (e-f)	6
SiO_2 + γ (e-f-j-k)	6, 7
*SiO_2 + $Li_2Si_2O_5$ + $MgSiO_3$ + γ (f)	6
SiO_2 + Zn_2SiO_4 s.s. (Zn_2SiO_4 – 1) + γ (j-k)	7
*SiO_2 + $MgSiO_3$ + Zn_2SiO_4 s.s. (1) + γ (k)	7
$MgSiO_3$ + Mg_2SiO_4 s.s. (m) + Zn_2SiO_4 s.s. (l) + γ (k)	7
$MgSiO_3$ + Mg_2SiO_4 s.s. (m-n) + γ (g-f-k)	7
$MgSiO_3$ + SiO_2 + γ (k-f)	7
*$MgSiO_3$ + $Li_2Si_2O_5$ + Li_2SiO_3 + γ (f)	8
Li_2SiO_3 + $MgSiO_3$ + γ (f-g)	8
*Li_2SiO_3 + $MgSiO_3$ + Mg_2SiO_4 s.s. (n) + γ (g)	8
Li_2SiO_3 + $MgSiO_3$ + Mg_2SiO_4 s.s. (Mg_2SiO_4 – n)	8
*Li_2SiO_3 + Mg_2SiO_4 s.s. (Mg_2SiO_4 – n) + γ (g-h)	8

Notes
*These volumes were observed experimentally.
Volumes containing $MgSiO_3$ neglect any solid solution of "$ZnSiO_3$" in $MgSiO_3$.
Compositions (mol % Li_4SiO_4:Zn_2SiO_4:Mg_2SiO_4):
a 82:18:0, b 70:0:30, c 75:25:0, d 60:0:40, e 50:50:0, f 50:30:20, g 50:22.5:27.5, h 50:0:50, j 32:68:0, k 33:52:15, l 0:79:21, m 0:18:82, n (est) 0:5-10:90:95.

compositions. All compositions containing > 66.7% SiO_2 will contain free SiO_2 as an equilibrium phase; Fig. 9 is simply a SiO_2 projection of these subsolidus volumes. The spatial positions of these volumes within the tetrahedron are found by projecting their outlines from the SiO_2 apex of the system onto the Li_2O-MgO-ZnO face. The corners of the triangular diagram, Fig. 9, and distances along the edges now represent bulk molar ratios of Li_2O:MgO:ZnO. The particular phase volume appropriate to any composition can be found by inspection, given the bulk molar ratios. The relative amounts of the phases within each volume can be found from auxiliary lever-rule calculations; examples are given in an Appendix.

Similar constructions may be used to calculate phase contents in compositions containing less SiO_2. Fig. 9 may also be used for many compositions containing between 50 and 66.7% SiO_2, especially those which fall into a volume which does not contain $Li_2Si_2O_5$. These compositions are found by inspection of Fig. 9. Because of the appearance of Li_2SiO_3 in some more basic compositions, those phase volumes shown in Fig. 9 which contain $Li_2Si_2O_5$ begin to contract at silica contents below 66.7% SiO_2. Fig. 10 shows

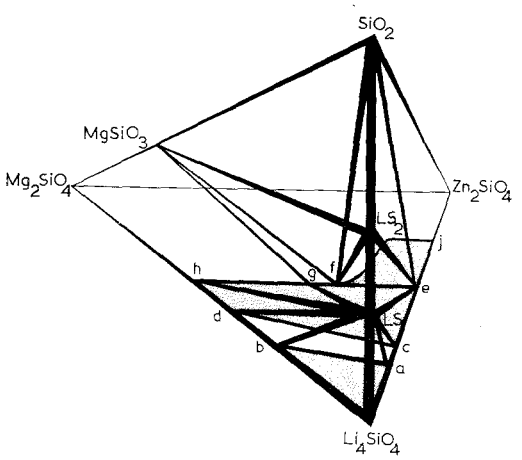

Figure 6 Subsolidus equilibria in part of the system Li_4SiO_4-Zn_2SiO_4-Mg_2SiO_4-SiO_2 at 800 to 850°C. The diagram is not drawn to scale. Solid solution compositions at the lettered points, given in mol% Li_4SiO_4:Zn_2SiO_4:Mg_2SiO_4 respectively, are:
a 82:18:0, b 70:0:30, c 75:25:0, d 60:0:40, e 50:50:0, f 50:30:20, g 50:22.5:27.5, h 50:0:50, j 32:68:0. Abbreviations: LS – Li_2SiO_3; LS_2 – $Li_2Si_2O_5$.

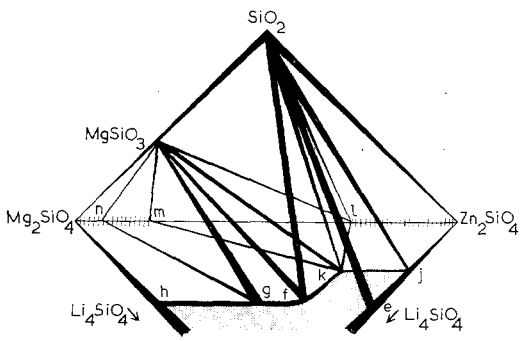

Figure 7 Subsolidus equilibria in part of the system Li_4SiO_4-Zn_2SiO_4-Mg_2SiO_4-SiO_2 at 800 to 850°C. Compositions of the lettered points a to j are given in the caption to Fig. 6; also: k 33:52:15, l 0:79:21, m 0:18:82, n 0:(5-10):(90-95).

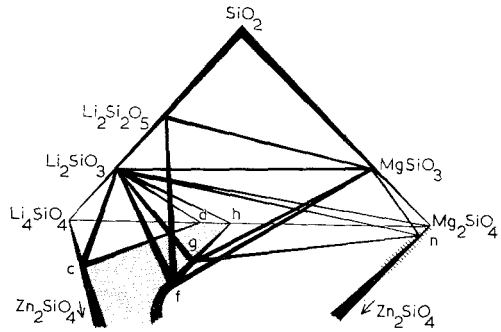

Figure 8 Subsolidus equilibria in part of the system Li_4SiO_4-Zn_2SiO_4-Mg_2SiO_4-SiO_2 at 800 to 850°C. Compositions of the lettered points are given in the captions to Figs. 6 and 7.

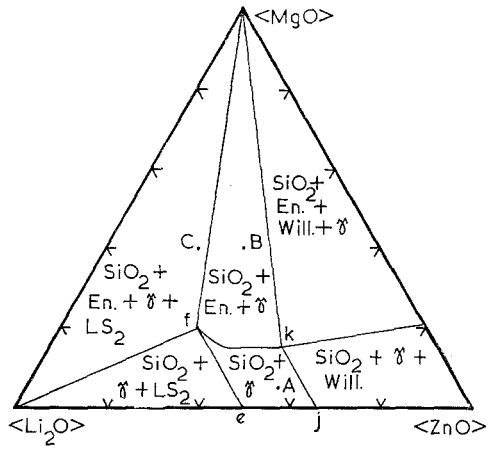

Figure 9 Subsolidus equilibria in the system Li_4SiO_4-Zn_2SiO_4-Mg_2SiO_4-SiO_2 at 800 to 850°C. The Li_2O, ZnO and MgO apices are enclosed: < >, to indicate that this is a projection of the quaternary phase relations, for compositions containing > 66.7% SiO_2, onto the Li_2O-ZnO-MgO face. Grid marks represent ratios of Li_2O:ZnO:MgO. Abbreviations: En – Enstatite ($MgSiO_3$), Will. – willemite (Zn_2SiO_4), LS_2 – $Li_2Si_2O_5$, γ – $Li_2(Zn, Mg)SiO_4$ solid solution. The phase compositions of the lettered points A, B and C are calculated in the appendix.

sections through the system at 60, 55 and 50% SiO_2 projected onto the Li_2O-MgO-ZnO face. It can be seen that volumes such as ($Li_2Si_2O_5$ + SiO_2 + γ) contract with decreasing SiO_2 content. In addition, volumes such as ($Li_2Si_2O_5$ + Li_2SiO_3 + γ), which do not extend to compositions containing > 66.7% SiO_2, expand with decreasing SiO_2 content.

A noteworthy feature of this system is the widespread occurrence of orthosilicate phases. All quaternary compositions will contain a γ-type orthosilicate phase at equilibrium and, in compositions containing > 66.7% SiO_2, a γ-orthosilicate will be compatible with SiO_2.

No account has been taken of the variation in composition of the magnesium metasilicate phase in constructing the quaternary volumes. However, the extent of this solid solution is only a few percent "$ZnSiO_3$" and ignoring the existence of this solid solution will affect only slightly the compositional limits of the phase volumes containing $MgSiO_3$ solid solutions. An interesting observation is that $MgSiO_3$ formed at subsolidus temperatures, either by reaction of

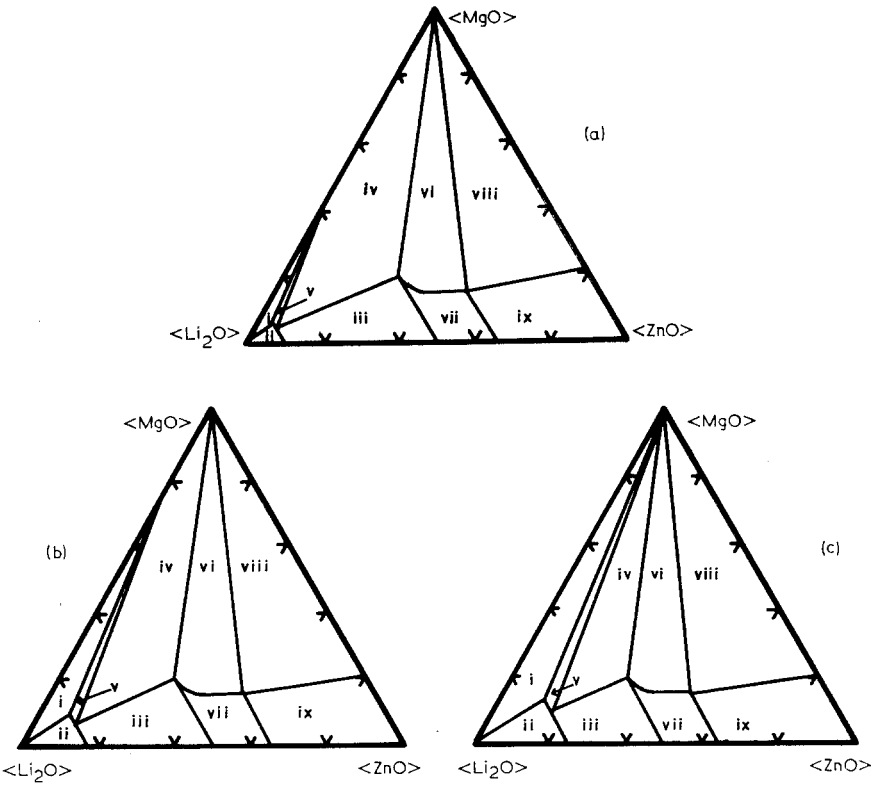

Figure 10 Subsolidus equilibria in the system Li_4SiO_4: Zn_2SiO_4: Mg_2SiO_4:SiO_2: sections through the system at 800 to 850° C for (a) 60 mol % SiO_2, (b) 55 % SiO_2, (c) 50 % SiO_2. Grid marks represent ratios of Li_2O:ZnO:MgO. Phases present in the numbered quaternary subsolidus volumes are as follows:
(i) $Li_2SiO_3 + MgSiO_3 + Li_2Si_2O_5 + \gamma$, (ii) $Li_2SiO_3 + Li_2Si_2O_5 + \gamma$, (iii) $Li_2Si_2O_5 + SiO_2 + \gamma$, (iv) $Li_2Si_2O_5 + MgSiO_3 + SiO_2 + \gamma$, (v) $Li_2Si_2O_5 + MgSiO_3 + \gamma$, (vi) $MgSiO_3 + SiO_2 + \gamma$, (vii) $SiO_2 + \gamma$, (viii) $SiO_2 + MgSiO_3 + Zn_2SiO_4$ ss. $+ \gamma$, (ix) $SiO_2 + Zn_2SiO_4$ ss $+ \gamma$.

crystalline starting materials or by crystallization of glasses, is preserved to ambient temperatures as orthorhombic enstatite.

3.5. Properties of some orthosilicate phases

3.5.1. Solubilities

The solubilities of Li_2ZnSiO_4 and Li_2MgSiO_4 in distilled water, 2N HCl and 2N NaOH were measured. Sintered lumps (about 0.5 to 1.0 g) of the orthosilicate were immersed for two to three days in approximately 200 ml of solvent boiling under reflux. If the sinters appeared to be unattacked by this treatment, they were dried and any weight change measured. The sinters or remaining solids were also examined by optical microscopy and X-ray powder diffraction.

(i) H_2O. Neither phase showed any signs of attack or leaching by boiling distilled water after three days.

(ii) 2N HCl. Although the sinters of both phases remained intact, they were microscopically isotropic and amorphous to X-rays. Complete leaching of the non-siliceous components had probably occurred.

(iii) 2N NaOH. The sinters of both phases had completely disintegrated after one to two days in boiling NaOH solution. X-ray powder diffraction showed the presence of ($Li_2ZnSiO_4(\gamma_0)$ + ZnO) and ($Li_2MgSiO_4(\gamma_0)$ + other unidentified phase(s)) respectively.

3.5.2. Thermal expansion

Directional coefficients of thermal expansion of Li_2MgSiO_4 were measured from high-temperature X-ray powder photographs. The calculated coefficients, shown in Table III, have values comparable to those obtained for Li_2ZnSiO_4 [2].

3.5.3. Electrical conductivities

Direct current electrical conductivities of sintered

TABLE III Unit-cell size and directional coefficients of thermal expansion of Li_2MgSiO_4

γ_0-Li_2MgSiO_4 ΔT:25° to 400°C		γ_{II}-Li_2MgSiO_4 ΔT:650 to 1020°C	
$d_{(200)}$ (Å)	3.17 3.19	3.21	3.23
$d_{(040)}$ (Å)	2.65 2.69	2.70	2.72
$d_{(002)}$ (Å)	2.50 2.52	2.53	2.55_5

Expansivity: $\alpha \times 10^{-5}$ °C^{-1}

Crystallographic direction	ΔT 25 to 400°C	ΔT 650 to 1020°C
a	1.7 ± 0.8	2.0 ± 1.0
b	3.7 ± 0.9	2.4 ± 1.2
c	2.0 ± 1.0	3.1 ± 1.2

cubes of Li_2MgSiO_4 and Mg_2SiO_4 were measured: results are shown in Fig. 11. Li_2MgSiO_4 and Mg_2SiO_4 have conductivities similar to Li_2ZnSiO_4 and Zn_2SiO_4 respectively [2].

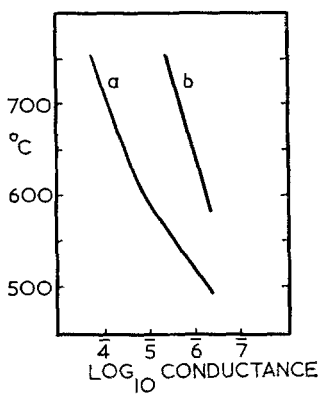

Figure 11 Direct current conductance measurements on some orthosilicate sinters. Curve (a) Li_2MgSiO_4; (b) Mg_2SiO_4.

3.6. Non-equilibrium crystallization of quaternary glasses

The approximate limits of glass formation in the Li_2O-ZnO-SiO_2 system (indicated in Fig. 12) do not cross the orthosilicate join; thus, all glasses whose crystallization are described below contain more than 50% SiO_2. These remarks also apply to "quaternary" glasses containing MgO.

The quaternary glasses may be crystallized over a range of temperatures to give a variety of products, both equilibrium and non-equilibrium. At temperatures just below the solidus, non-equilibrium phases may crystallize initially, but these soon react or decompose to give the equilibrium phase assemblages. However, with falling

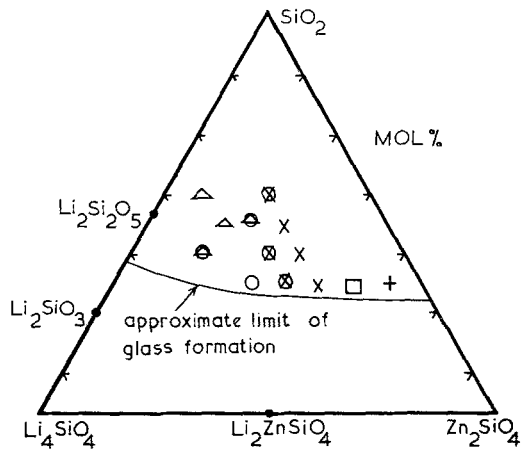

Figure 12 The system Li_4SiO_4-Zn_2SiO_4-SiO_2 showing the approximate limit of glass formation (for 1 to 2 g of melt quenched in a Pt crucible). Some compositions close to the ZnO-SiO_2 edge exhibit stable liquid immiscibility. The first products of glass crystallization at 550 to 650°C are indicated: Δ, metastable solid solutions of SiO_2 in $Li_2Si_2O_5$: zinc may also be present in solid solution; O, metastable Proto-β phase; X, metastable β_{II} lithium zinc orthosilicate having a variable Li_2O:ZnO ratio and which may contain an excess of SiO_2 in solid solution, □, metastable γ_{II} lithium zinc orthosilicate: may contain an excess of SiO_2 in solid solution; +, metastable β-zinc silicate: composition unknown.

temperatures, departures from equilibrium are increasingly observed and progressively longer heating times are required in order to attain equilibrium. The overall crystallization kinetics become very complex. The effects of changing both temperature and bulk composition are frequently to alter the paths of crystallization, as well as the phases obtained.

The general sequences of phases obtained in compositions on the join Li_4SiO_4-Zn_2SiO_4, as a function of cooling rate from about 1000°C, are

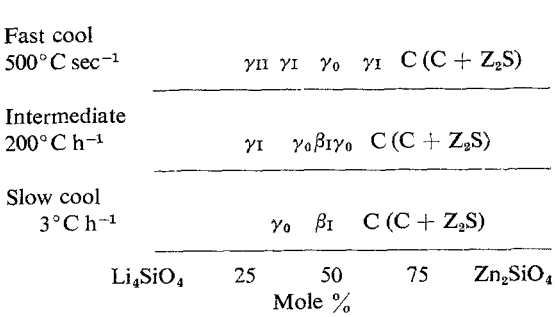

Figure 13 Guide to the phases obtained at ambient, on cooling lithium zinc orthosilicate compositions from about 900°C at the rates indicated.

shown in Fig. 13. This serves as a simple and approximate guide to the occurrence of orthosilicate phases in quaternary compositions, for two reasons. Firstly, the presence of additional phases, e.g. SiO_2 or $Li_2Si_2O_5$, does not alter the sequence of orthosilicate phase transformations which are observed under equilibrium or reversible non-equilibrium conditions. Secondly, partial substitution of Zn^{2+} by Mg^{2+} does not markedly alter the general sequence of transformations shown in Fig. 13 until comparatively high Mg:Zn ratios (about 0.3:0.7) are reached, and orthosilicates of such high Mg-content crystallize from only a restricted range of glass-forming compositions.

However, quaternary glasses show several other important metastable features of crystallization. Some of these features involve orthosilicates and phases of related composition. A hexagonal phase with the wurtzite (ZnS) structure is a commonly-occurring first product of crystallization of many glasses, as shown in Fig. 12. The X-ray powder patterns of this phase named "Proto-β", are usually diffuse indicating the crystals to be very small; microscopically, glass which has crystallized Proto-β is often still isotropic and apparently non-crystalline. Electron diffraction patterns of some of the Proto-β containing specimens were obtained, and although single crystals of Proto-β were not isolated, there was no evidence of superstructure reflections. Glasses having an Li_2O:ZnO ratio of 1:1 gave Proto-β as the only crystalline product at 550 to 600°C, but more lithia-rich compositions, e.g. those having an Li_2O:ZnO ratio of 3:1, yielded lithium disilicate solid solutions in addition to Proto-β. The range of zinc-rich glasses yielding Proto-β is much more restricted and it was never obtained from glasses having Li_2O:ZnO ratios $\leqslant$ 3:4. In the quaternary system, a series of glasses of approximately metasilicate composition, and having an Li_2O:(Zn + Mg)O ratio of 1:1, all yielded Proto-β at 550 to 600°C: the more magnesium-rich glasses also yielded some lithium disilicate. A typical powder X-ray pattern is shown in Table IV. The variation in X-ray d-spacings of these Proto-β solid solutions as a function of the Zn-Mg ratio of the glass starting materials, is shown in Fig. 14.

The exact compositions of Proto-β are not known. Although its X-ray powder pattern suggests that it has a wurtzite-like structure, it is not simply ZnO. Its hexagonal unit cell dimensions, especially a_0, differ considerably from those of ZnO: for Proto-β, a_0 ranges from 2.67 to 2.70Å: for ZnO, a_0 = 2.816Å.

TABLE IV X-ray powder diffraction data for proto-β lithium zinc silicate

d(Å)	I	hkl
2.68	100	100
2.47	60	002
2.36	20	101
1.81	30	102
1.54	40	110
1.31	10	

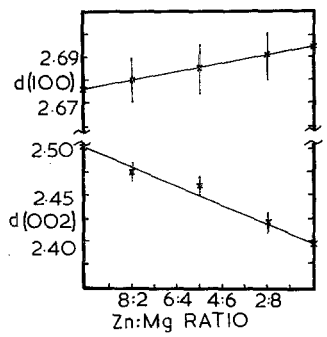

Figure 14 Variation of $d_{(100)}$ and $d_{(002)}$ (in Å) of the Proto-β phase with the zinc : magnesium ratio of the parent lithium zinc magnesium silicate glasses. The compositions of the Proto-β phase itself are unknown.

Proto-β is very similar to a hexagonal phase which has been observed to crystallize from lithium aluminosilicate glasses [9]. This phase was described as "a polymorph of $LiAlO_2$ with a variable degree of solid solution of SiO_2 and also some variation in the Li/Al ratio". Thus it appears to be of widespread occurrence as an early crystallization product in Li_2O-SiO_2 systems which contain other small cations such as Zn, Mg or Al. In the present case, the Proto-β contains essential Li, Mg, Zn and silicon. It is believed to have a hexagonal close-packed oxygen arrangement, like that of ZnO, with Li, Zn, Mg and Si disordered over the same set of tetrahedral cation sites as are occupied in ZnO.

All Proto-β containing samples give relatively diffuse X-ray powder patterns. On heating at about 650°C, the patterns sharpen and superstructure reflections appear as Proto-β converts gradually to β_{II}. In structural terms, this transformation involves partial cation ordering. By analogy with the cation distribution in β_{II} lithium zinc silicate and its isotype, low-Li_3PO_4, the silicons become ordered on every fourth

cation site, while the other cations remain disordered. β_{II} prepared in this way is readily preserved to ambient. This contrasts with β_{II} prepared from Li_4SiO_4-Zn_2SiO_4 (Fig. 13), or Li_4SiO_4-Zn_2SiO_4-Mg_2SiO_4 compositions where β_{II} may be formed at higher temperature but cannot be preserved to ambient; it instead undergoes one or more minor phase transformations on cooling. The metastable β_{II} crystallized from glass is believed to contain an excess of SiO_2, relative to the "ideal" orthosilicate ratio. Upon heating to about 700°C, it decomposes; the decomposition products depend upon composition (Fig. 13), but include β-, γ- and C-type phases, and crystalline SiO_2 makes its first appearance in many compositions. Crystallization at about 600°C of progressively more zinc-rich glasses (shown in Fig. 12) yields β_{II} and γ_{II} respectively, as the first crystalline products. Again, β_{II} and γ_{II} are readily retained metastably to ambient and are believed to contain an excess of silica in solid solution.

Crystallization of ZnO-SiO_2 glasses and melts has been shown to produce a metastable β-zinc silicate phase of varying composition as an early crystallization product [10]. However, the non-equilibrium features of the ZnO-SiO_2 and also, of the MgO-SiO_2 systems are not readily amenable to study because of their high liquidus temperatures (> 1450°C) and the small range of compositions which yield glasses easily. In the present study, a β-zinc silicate phase has been observed to crystallize from lithium zinc silicate glasses containing up to 5 to 10% Li_2O.

Lithium disilicate solid solutions have been observed to form as an early product of crystallization from the compositions shown in Fig. 12. Although $Li_2Si_2O_5$ is a stable phase, and one which appears at equilibrium in many of the quaternary subsolidus assemblages, its solid solutions are metastable. These metastable solid solutions may contain an excess of either lithium or silicon; their compositions extend from 62 to 72 mol % SiO_2. The lithia-rich solid solutions decompose readily upon heating by exsolution of Li_2SiO_3. The silica-rich solid solutions are more resistant to decomposition. An interpretation of the X-ray powder patterns and their use and limitations in finding the composition of the solid solutions in the Li_2O-SiO_2 system has been discussed previously [8]. A few experiments have been done on the crystallization of lithium zinc silicate glasses around the lithium disilicate composition but having SiO_2:Li_2O ratios > 2:1. The results show that, if variations in the X-ray *d*-spacings can be interpreted as arising only from changes in the Li_2O:SiO_2 ratio, the disilicate phase crystallizing between about 550 and 700° from these silica-rich glasses contains an excess of silica in solid solution. The effect of raising the temperature to about 740°C is to cause the *d*-spacings of the disilicate phase to return to those of approximately $Li_2Si_2O_5$ and crystalline silica to appear. It is feasible that the disilicate phase will also take some zinc metastably into solid solution; although no direct X-ray evidence was obtained to support this possibility, only glasses containing > 10% ZnO readily crystallized an additional phase, a β-type orthosilicate, below about 650°C,

The effects of Li^+ and Zn^{2+} on the crystallization of the $MgSiO_3$ phase are also of possible importance. $MgSiO_3$ has been observed to crystallize from glasses as the orthorhombic form. Rhombic enstatite is, in fact, the stable phase up to about 900°C, but the usefulness of $MgSiO_3$ as a ceramic phase is often limited by its tendency to crystallize first as protoenstatite which subsequently undergoes a series of troublesome conversion reactions.

Acknowledgement

A.R.W. was supported by a University Studentship from the Robbie, Japp and Coutts funds. The Science Research Council provided funds for equipment and materials.

Appendix

In order to make the fullest use of the data given here, it is desirable to be able to convert from bulk chemical composition to phase composition. Three examples of the calculations will be given for compositions containing > 66.7% SiO_2 and which fall into two-, three- and four-phase subsolidus compatibility volumes.

Example A. Composition: 80% SiO_2, 8% Li_2O, 1% MgO, 11% ZnO. The molar ratio Li_2O:MgO:ZnO for this composition is 8:1:11. The composition projects in Fig. 9 at point A, and upon complete crystallization at about 850°C, yields a two-phase mixture of γ-ortho silicate and SiO_2 (quartz). Since the quartz is virtually pure and the orthosilicate contains 33.3% SiO_2, the mole fraction of SiO_2 is, from the lever-rule: $(80 - 33.3)/(100 - 33.3) \cong 0.7$. The remaining 0.3 mole fraction is a homogeneous γ-orthosilicate solid solution whose composition has the empirical formula $8Li_2O$.

$MgO.11ZnO.10SiO_2$.

Example B. Composition: 80% SiO_2, 6% Li_2O, 8% MgO, 6% ZnO. The molar ratio of Li_2O:MgO:ZnO is 3:4:3. This ratio projects in Fig. 9 at point B, and upon complete crystallization at about 850°C, yields a three-phase mixture of SiO_2, $MgSiO_3$ and a γ-orthosilicate solid solution The Li_2O:MgO:ZnO ratios of the orthosilicate solid solutions which are present in this phase volume are variable and fall upon the curve fk. For a particular bulk composition such as B, the orthosilicate composition can be found by extending a line from the ⟨MgO⟩ apex, through point B to its intersection with the curve fk. In this example, the oxide molar ratios in the orthosilicate are thus estimated as $(Li_2O)_{42.5}$: $(MgO)_{15}$:$(ZnO)_{42.5}$, giving an orthosilicate solid solution of formula $Li_{1.7}Mg_{0.3}Zn_{0.85}Si_{1.0}O_{4.0}$. It is, therefore, non-stoichiometric with respect to the "ideal" composition, $Li_2(Mg, Zn)SiO_4$. All the lithia enters the orthosilicate, so that, per 100 moles of reactants, 7.0 moles of this solid solution are formed. To form this quantity requires 6 moles of Li_2O, 2.1 moles MgO, 6.0 moles ZnO and 7.0 moles SiO_2. The remaining MgO (8 − 2.1), or 5.9 moles, reacts with an equivalent molar quantity of SiO_2 to form 5.9 moles of $MgSiO_3$. The remaining SiO_2 is now 80 − (7.0 + 5.9) or 67 moles. Thus, this composition contains, at equilibrium, 67 moles of SiO_2, 7 moles of γ-orthosilicate and about 6 moles of $MgSiO_3$. This corresponds to an overall phase composition of 0.84 mole fraction SiO_2, 0.07 $MgSiO_3$ and 0.09 γ-orthosilicate.

Example C. Composition: 80% SiO_2, 8% Li_2O, 8% MgO, 4% ZnO. The molar ratio of Li_2O:MgO:ZnO is 2:2:1. This ratio projects in Fig. 9 at point C, and upon complete crystallization at about 850°C, yields a four-phase mixture of SiO_2, $MgSiO_3$, $Li_2Si_2O_5$ and a γ-orthosilicate solid solution. The principle of the calculation is basically the same as that used in Example B. In a four-phase equilibrium, however, the composition of the γ-orthosilicate phase will be fixed at any one temperature. Therefore, this (as well as other compositions lying within this volume) will yield a γ-orthosilicate whose composition lies at point f and which corresponds to $Li_2Zn_{0.6}Mg_{0.4}SiO_4$. The quantity of γ-phase at equilibrium can be calculated from the amount of zinc, since all the zinc is in the γ-phase. The remaining magnesium will all be in the $MgSiO_3$ phase and likewise the remaining lithium will all be in $Li_2Si_2O_5$. The silica not utilized in the formation of one of these three phases will occur as free quartz.

References

1. A. R. WEST and F. P. GLASSER, *J. Mater. Sci.* **5** (1970) 557.
2. *Idem, ibid* **5** (1970) 676.
3. *Idem, ibid* **6** (1971) 1100.
4. I. M. STEWART and G. J. P. BUCHI, *Trans. Brit. Ceram. Soc.* **61** (1962) 615.
5. A. H. LAM, Ph.D. Thesis, "Phase Equilibria and Crystallization of the Lithia-Zinc Oxide-Silica System", University of Sheffield (1964).
6. F. A. HUMMEL and M. KRISHNA MURTHY, *J. Amer. Ceram. Soc.* **38** (1955) 55.
7. E. R. SEGNIT and A. E. HOLLAND, *ibid* **48** (1965) 405.
8. A. R. WEST and F. P. GLASSER, submitted to "Symposium on Nucleation and Crystallization in Glasses and Melts", *Amer. Ceram. Soc.* (1971).
9. T. I. BARRY, D. CLINTON, L. A. LAY, R. A. MERCER, and R. P. MILLER, *J. Mater. Sci.* **5** (1970) 117.
10. J. WILLIAMSON and F. P. GLASSER, *Phys. Chem. Glasses* **5** (1964) 52.

Received 14 September 1971 accepted in revised form 19 January 1972.